

Calibration-independent consistency test of DESI DR2 BAO and SNIa

Bikash R. Dinda^{a,b} , Roy Maartens^{a,b} , Chris Clarkson^{c,a}

^aDepartment of Physics & Astronomy, University of the Western Cape, Cape Town 7535, South Africa

^bNational Institute for Theoretical & Computational Science, Cape Town 7535, South Africa

^cDepartment of Physics & Astronomy, Queen Mary University of London, London E1 4NS, United Kingdom

E-mail: bikashrdinda@gmail.com, rmaartens@uwc.ac.za, chris.clarkson@qmul.ac.uk

Abstract. We investigate the consistency between DESI DR2 BAO and three SNIa datasets, Pantheon+, Union3, and DES-Y5. Our consistency test is calibration-independent since it is independent of cosmological nuisance parameters such as the absolute peak magnitude M_B and the comoving sound horizon at the baryon drag epoch r_d . This could reduce some systematics in the observed data, if present. Importantly, the test is also model-agnostic, independent of any model of dark energy or modified gravity. We define a tension parameter to quantify tension across different datasets compared to DESI DR2 BAO. The Pantheon+ and Union3 data have tension $\lesssim 1\sigma$ across their redshift ranges, whereas the DES-Y5 tension is $\gtrsim 3\sigma$ near $z = 1$. This hints that DES-Y5 data has significant offset values for redshifts close to 1, compared to the other SNIa datasets. Since this consistency test is independent of cosmological nuisance parameters, the tension is minimal: other consistency tests involving differences in nuisance parameters may show greater tension.

Contents

| | | |
|----------|--|----------|
| 1 | Introduction | 1 |
| 2 | Data related observables | 2 |
| 3 | Results | 3 |
| 4 | Conclusions | 4 |
| A | Gaussian Processes and m_B, μ_B | 5 |
| B | Robustness of the results | 6 |
| C | Effects of cosmic curvature in the consistency test | 6 |
| D | Potential consequences of the consistency test | 7 |
| D.1 | Violation of cosmic distance duality relation | 7 |
| D.2 | Violation of standard candle assumptions | 8 |

1 Introduction

Data Release 2 (DR2) of the Dark Energy Spectroscopic Instrument (DESI) has provided unprecedented constraints on cosmic distance measurements through baryon acoustic oscillation (BAO) observations [1]. Specifically, when analyzed through $w_0 w_a$ parameterizations of the dark energy equation of state $w(z)$, and in combination with cosmic microwave background (CMB) [2, 3] and type Ia supernova (SNIa) [4–6] datasets, it gives hints of dynamical dark energy, including a possible phantom crossing ($w < -1$) [1, 7].

The SNIa observations, from Pantheon+ [4], Union3 [5], and Dark Energy Survey Year 5 (DES-Y5) [6], play a crucial role in tightening constraints, especially on the low-redshift dark energy behavior and as a whole on the late-time expansion of the Universe. Dynamical dark energy would signal a major change to the standard model of cosmology. Phantom behavior of dark energy is a further potential challenge to general relativity, pointing towards the possibilities of an interacting dark sector or modified gravity (e.g. [8–14]). In light of these major possibilities, it is important in particular to check the consistency across the data sets [15, 16]. Since tighter constraints at low redshifts are obtained from the combination of DESI DR2 BAO and SNIa (with CMB), and since both kinds of observations share a significant redshift range, consistency in these ranges must be checked [17–22].

The consistency check between BAO and SNIa is not straightforward because they do not really measure the same observables. BAO observations provide uncalibrated cosmological distances, and to obtain the actual distance, we need to calibrate with the comoving sound horizon at the baryon drag epoch r_d . In order to put the supernova observables (apparent peak magnitude m_B) on the same footing (cosmological distance, such as the luminosity distance d_L), we need to calibrate the SNIa observations with the absolute peak magnitude M_B . This means that the results of the consistency check depend on these nuisance parameters [23–27]. Consequently, in order to check the actual consistency, we need either to marginalize over

the nuisance parameters or to consider tests that are entirely independent of the nuisance parameters.

In this analysis, we test the consistency between the DESI DR2 BAO and SNIa observations, independent of these nuisance parameters, that is, independent of the calibration. This consistency test ensures that to test consistency, we do not need any third kind of observations, such as CMB for r_d or local distance observations for M_B .

2 Data related observables

BAO observations are related to the important Alcock–Paczynski (AP) variable,

$$F_{\text{AP}}(z) = \frac{D_M(z)}{D_H(z)} = \frac{\tilde{D}_M(z)}{\tilde{D}_H(z)}, \quad (2.1)$$

where D_M and D_H are the comoving and Hubble distances, respectively, and $\tilde{D}_M = D_M/r_d$ and $\tilde{D}_H = D_H/r_d$ are the uncalibrated distances. The distance modulus in SNIa observations is

$$\mu_B(z) = m_B(z) - M_B = 5 \log_{10} \left[\frac{d_L(z)}{\text{Mpc}} \right] + 25 \quad \text{where} \quad d_L(z) = (1+z)D_M(z). \quad (2.2)$$

Here, m_B and M_B are the apparent and absolute peak magnitudes of SNIa, respectively. We can rearrange this to express D_M in terms of m_B or μ_B :

$$D_M(z) = \alpha A(z) = \beta B(z) \quad \text{with} \quad \alpha = e^{-b(5+M_B)} \text{ Mpc}, \quad b = \frac{\ln(10)}{5}, \quad \beta = 1 \text{ Gpc}, \quad (2.3)$$

and where

$$A(z) = (1+z)^{-1} \exp \left\{ b[m_B(z) - 20] \right\}, \quad B(z) = (1+z)^{-1} \exp \left\{ b[\mu_B(z) - 40] \right\}. \quad (2.4)$$

In the flat FLRW background, $D_H = D'_M$, where a prime is a redshift derivative. Then the derivative of [Equation 2.3](#) leads to

$$F_{\text{AP}}(z) = \frac{A(z)}{A'(z)} = \frac{B(z)}{B'(z)}. \quad (2.5)$$

It follows that F_{AP} depends only on m_B or μ_B and is independent of M_B . Writing F_{AP} in terms of A and B allows us to handle the SNIa data given in m_B or μ_B . It may seem unnecessary to express F_{AP} in new variables A, B rather than m_B, μ_B , where $F_{\text{AP}}(z) = (1+z)/[b(1+z)m'_B(z) - 1] = (1+z)[b(1+z)\mu'_B(z) - 1]$. The reason is that there are subtle differences when we apply GP. In [Appendix A](#), we show that it is better to apply GP to A, B than to m_B, μ_B .

BAO observations from DESI DR2 directly provide data for F_{AP} . In addition, we consider three SNIa datasets: Pantheon+, Union3, and DES-Y5. The first two have data up to redshift $z \sim 2.4$, whereas the third reaches $z \sim 1.2$. SNIa observations provide data of m_B in Pantheon+ and DES-Y5, but Union3 has not officially released actual data, providing only binned μ_B data. As mentioned above, this is not an issue in our case, since our methodology applies to both m_B and μ_B . This is the reason we write D_M in terms of A and B in [Equation 2.3](#). We directly convert these SNIa data to A and B data, using [Equation 2.4](#) with uncertainty predictions (including both self- and cross-variances). These are shown in [Figure 1](#) (black data points).

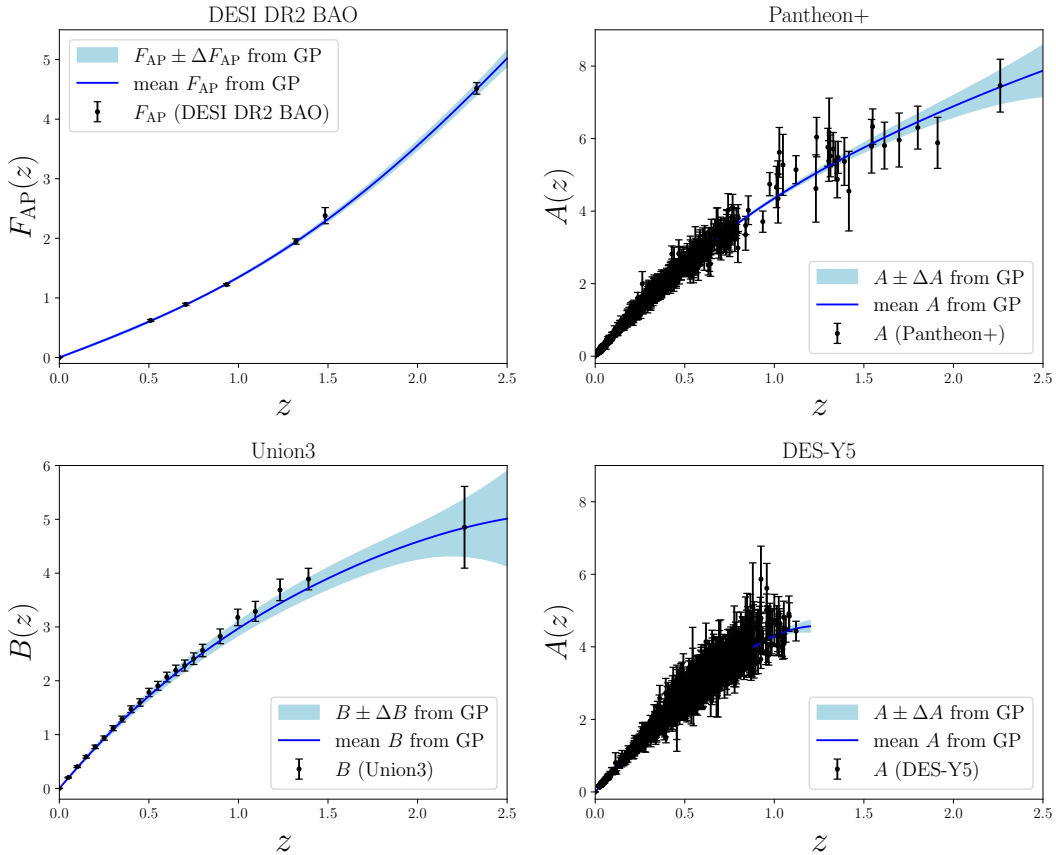


Figure 1. Gaussian Process predictions (blue) compared to observational data (black), where A and B are defined in Equation 2.4.

3 Results

We apply GP to the DESI DR2 F_{AP} data directly in order to reconstruct a smooth function and the associated uncertainties. For this purpose, we consider a zero-mean function and a squared-exponential kernel covariance function. Similarly, we apply GP to A (Pantheon+ and DES-Y5) and B (Union3) data, to reconstruct these and their first derivatives. The results are shown in Figure 1 for a visual test of the accuracy of GP regression predictions (blue curves) compared to the actual data (black data points).

In order to check the robustness of the results, we show in Appendix B that the GP reconstructed results are compatible with 4th and 5th-order polynomial reconstructed results.

Using these GP predicted smooth functions and their derivatives (wherever needed), we compute $F_{\text{AP}}(z)$. We compare these to the DESI data in the left panel of Figure 2, which displays the ratios of the SNIa F_{AP} and the DESI F_{AP} . The shading shows the 1σ errors on these ratios. At lower redshifts ($z < 0.3 - 0.4$) all three SNIa datasets are $\sim 1\sigma$ away from the DESI DR2 BAO data. In the middle redshift range ($0.3 - 0.4 < z < 1.15$), we see that the discrepancy between DESI DR2 BAO, Pantheon+, and Union3 is decreasing to less than 1σ . However, the DES-Y5 data show a strong growth in inconsistency with DESI DR2 BAO. In the highest redshift range, where there is no DES-Y5 data, we see that the inconsistency for Pantheon+ and Union3 decreases even further, well within 1σ .

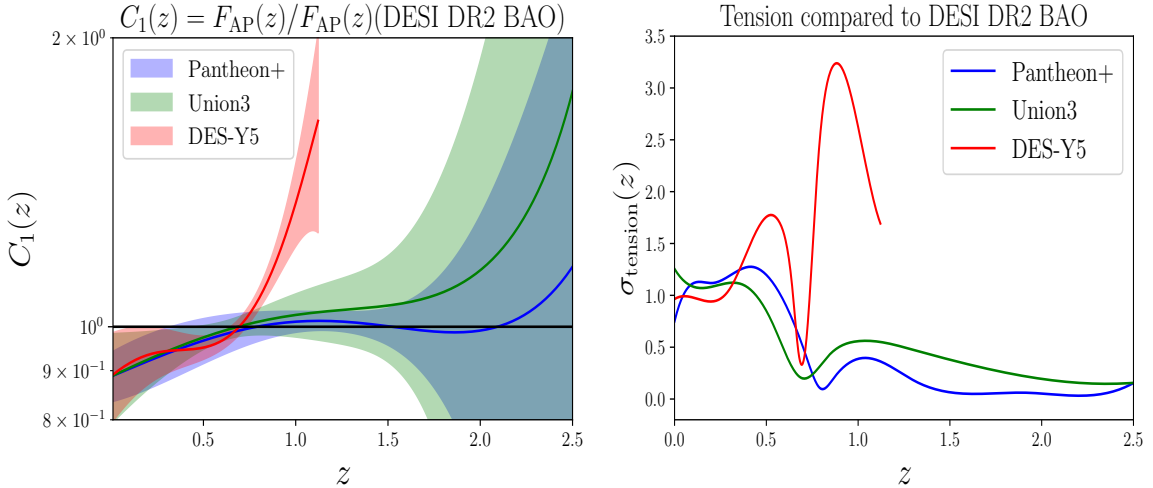


Figure 2. *Left:* F_{AP} comparison of SNIa data to DESI data. *Right:* Tension between SNIa and DESI datasets, as given by Equation 3.1.

In order to properly quantify the inconsistency across different observations, we define a tension parameter in units of 1σ confidence intervals:

$$\sigma_{\text{tension}}(z) = \frac{|F_{\text{AP}}(z) - F_{\text{AP}}(z)(\text{DESI DR2 BAO})|}{\left\{ [\Delta F_{\text{AP}}(z)]^2 + [\Delta F_{\text{AP}}(z)(\text{DESI DR2 BAO})]^2 \right\}^{1/2}}. \quad (3.1)$$

We display this tension parameter in the right panel of Figure 2. It is clear that the inconsistencies of Pantheon+ and Union3 with DESI DR2 BAO are around 1σ for $z \lesssim 0.5$ and decrease with increasing redshift for $z \gtrsim 0.5$. DES-Y5 data has similar low inconsistency for $z \lesssim 0.5$, but the inconsistency increases for $z \gtrsim 0.5$, up to more than 3σ near $z = 1$. DES-Y5 data have significantly offset values near $z = 1$, compared to Pantheon+ and Union3 data.

We assumed a spatially flat FLRW spacetime for these results. The relation in Equation 2.5 is modified by cosmic curvature, but curvature hardly makes any change to the results in the consistency test, as shown in Appendix C.

4 Conclusions

We presented a method for testing different datasets, which is independent of cosmological nuisance parameters, such as the peak absolute magnitude of SNIa. This consistency test is also model-agnostic.

We find DESI DR2 BAO, Pantheon+, and Union3 data are at around 1σ tension for $z \lesssim 0.5$, but decreasing for $z > 0.5$. The DES-Y5 data is consistent with the other two SNIa datasets at $z \lesssim 0.5$, but notably for $0.5 \lesssim z \lesssim 1.15$, the inconsistency increases, reaching more than 3σ near $z = 1$. DES-Y5 data is significantly offset in this redshift range – and this inconsistency is independent of M_B . The differences in M_B may even increase the inconsistency. This offset might have significant effects on the constraints on dark energy. We showed that the spatial curvature of the universe does not affect these conclusions.

If the mismatch between F_{AP} from BAO and from SNIa (using Equation 2.5) is not due to any systematic errors, this could hint at fundamental violations, such as: breakdown of

the cosmic distance duality relation, i.e. $d_L = (1+z)^2 d_A$, where d_A is the angular diameter distance; violation of the standard candle assumptions for SNIa; violation of the FLRW geometry of spacetime or of standard cosmic physics. We briefly discuss this in [Appendix D](#).

Acknowledgments

BRD and RM are supported by the South African Radio Astronomy Observatory and the National Research Foundation (Grant No. 75415).

A Gaussian Processes and m_B, μ_B

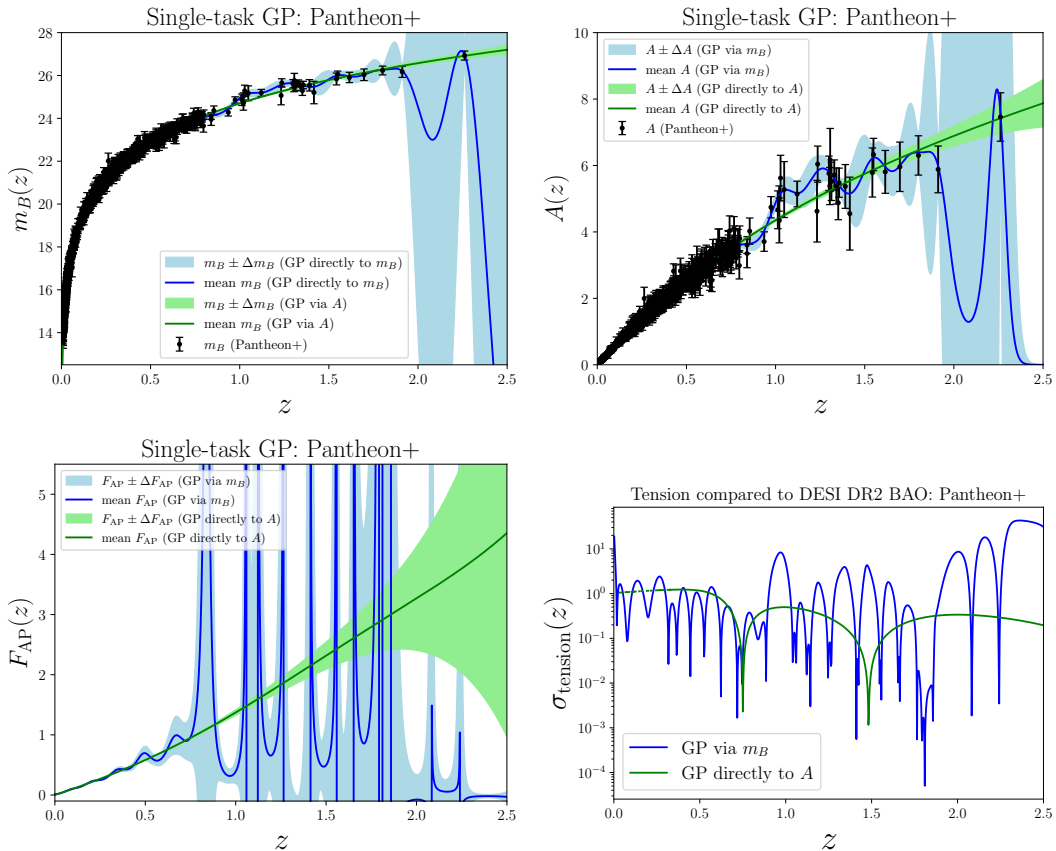


Figure 3. GP applied to m_B compared to A , using Pantheon+ data.

We used A, B instead of m_B, μ_B because the former variables lead to much smoother reconstructions. For example, the behavior of $m_B = 20 + \log[(1+z)A]/b$ is more nonlinear in z than A , even though it is derived from the same data (Pantheon+ or other SNIa data). When we apply GP to m_B , the value of the hyperparameter of the squared-exponential kernel is $l = 0.13$, significantly lower than $l = 2.44$ in the case of A . The lower l value means the reconstructed function changes more rapidly, with oscillations. Not only m_B , but also its derivatives are more oscillating due to the lower l . This is shown in [Figure 3](#). Clearly better results follow from applying GP to A than to m_B . This is also true for DES-Y5 data and Union3 data. Similarly, GP reconstruction of B is better behaved than that of μ_B . All these

points apply to a zero-mean function or a mean function that is not very close to the actual true underlying model of the data. More detailed investigation of these features is beyond the scope of this paper.

The same conclusions apply for polynomial regression (see [Appendix B](#)) as for GP.

B Robustness of the results

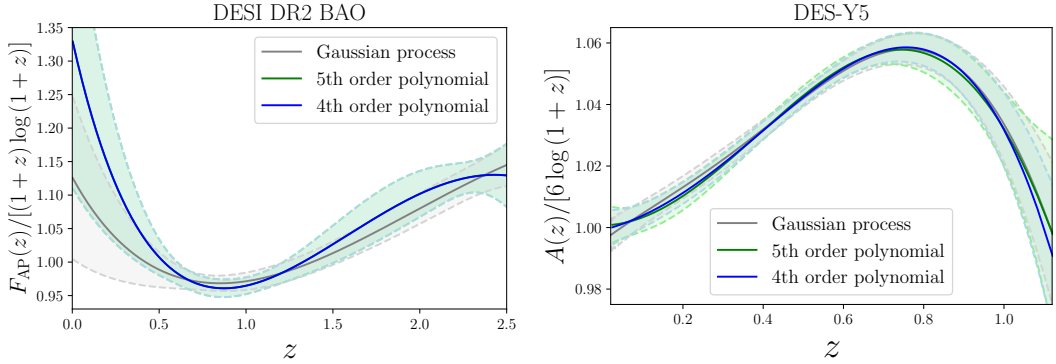


Figure 4. Robustness of the results.

To test the robustness of the results, we compare the GP reconstructed values to the 4th and 5th-order polynomial regression fitted values of the main functions. We see in [Figure 4](#) that the results agree with each other well within 1σ . We show this for DESI DR2 BAO (left) and DES-Y5 (right) data, but it is also true for the other two SNIa datasets.

C Effects of cosmic curvature in the consistency test

In curved spacetime, $\tilde{D}'_M \neq \tilde{D}_H$ [\[28\]](#):

$$\tilde{D}'_M = \tilde{D}_H \left[1 + \gamma \tilde{D}_M^2(z) \right]^{1/2} \quad \text{where} \quad \gamma = \Omega_{K0} \left(\frac{H_0 r_d}{c} \right)^2. \quad (\text{C.1})$$

Using this and [Equation 2.3](#), we find the connection between SNIa and BAO observables in general in curved spacetime:

$$\frac{A(z)}{A'(z)} = \frac{B(z)}{B'(z)} = F_{AP}(z) \left[1 + \gamma \tilde{D}_M^2(z) \right]^{-1/2}. \quad (\text{C.2})$$

DESI or any BAO observations provide both \tilde{D}_M and \tilde{D}_H . Then any reconstruction technique, such as GP or polynomial regression used here, which predicts derivatives (\tilde{D}'_M) along with the main function (\tilde{D}_M), allows us to find model-independent reconstruction of γ using [Equation C.1](#), alongside the main reconstructions. We use multi-task GP, extending the methodology for nonzero cosmic curvature in [\[29\]](#), to DESI DR2 BAO data, and we find that

$$\text{DESI DR2 BAO: } \gamma = (0.5 \pm 6.5) \times 10^{-5}.$$

The curvature correction term $|\gamma| \tilde{D}_M^2(z)$ is shown in [Figure 5](#) with associated 1σ uncertainties. It increases from zero (at $z = 0$) to a maximum $\sim 10^{-2}$ at $z = 2.5$, i.e. $|\gamma| \tilde{D}_M^2(z) \ll 1$

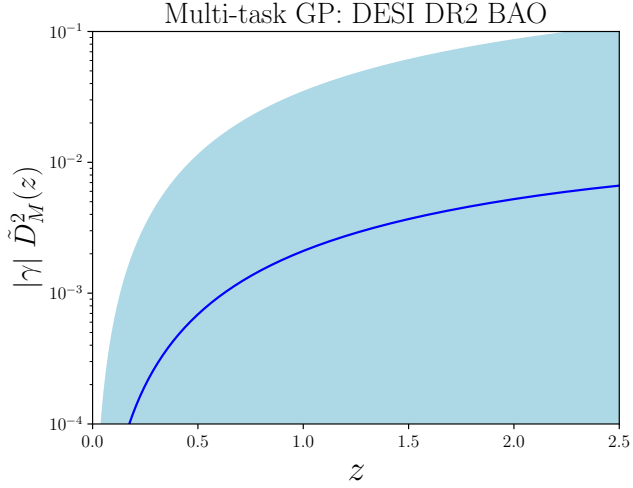


Figure 5. The curvature correction term $|\gamma|\tilde{D}_M^2(z)$.

for this entire redshift range. Consequently, there are negligible effects of cosmic curvature in our consistency test. However, $|\gamma|\tilde{D}_M^2(z)$ continues to increase for higher redshifts $z > 2.5$, because \tilde{D}_M increases with increasing redshift. Eventually, at a high enough redshift, the term becomes comparable to unity, and then cosmic curvature shows its effect. For this reason, curvature has effects on the CMB angular scales, but not in the setup considered here. Significant constraints on cosmic curvature come only when we include CMB data in any cosmological data analysis, e.g., as in Table V of [1], unless any future low redshift observations provide a significant value of γ comparable to 10^{-2} or larger.

D Potential consequences of the consistency test

If the mismatch between BAO and SNIa is not due to systematics, this could be a violation of standard physics. We consider two possibilities.

D.1 Violation of cosmic distance duality relation

We introduce a violation parameter η in Equation 2.2:

$$m_B(z) = M_B + 5 \log_{10} \left[\frac{\eta(z)(1+z)D_M(z)}{\text{Mpc}} \right] + 25, \quad (\text{D.1})$$

which leads to

$$\eta(z) = \frac{\exp \left\{ b[m_B(z) - M_B - 25] \right\}}{(1+z)D_M(z)} = \frac{\alpha A(z)}{r_d \tilde{D}_M(z)} = \frac{\beta B(z)}{r_d \tilde{D}_M(z)}, \quad (\text{D.2})$$

using Equation 2.3, Equation 2.4 and $\tilde{D}_M = D_M/r_d$. This can be rewritten as

$$\frac{r_d \eta}{\alpha} = \frac{A}{\tilde{D}_M} \quad \text{comparison between DESI DR2 BAO and Pantheon+ or DES-Y5}, \quad (\text{D.3})$$

$$\frac{r_d \eta}{\beta} = \frac{B}{\tilde{D}_M} \quad \text{comparison between DESI DR2 BAO and Union3}. \quad (\text{D.4})$$

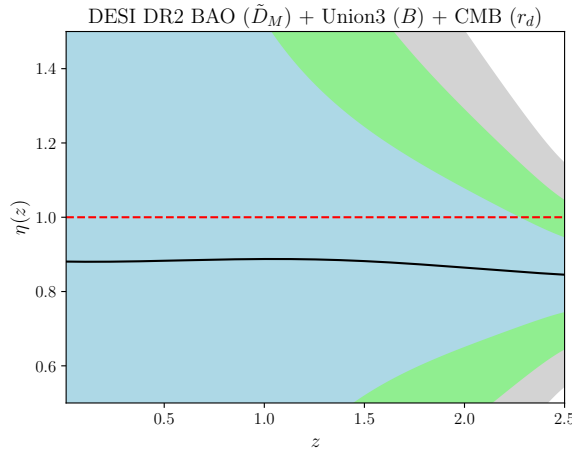


Figure 6. η obtained by combining DESI DR2 BAO, Union3 and CMB.

These two equations show that η is completely degenerate either with r_d (for Union3) or with r_d and M_B (for Pantheon+ or DES-Y5). In order to test the cosmic distance duality relation, we use r_d from CMB observations, assuming no violation of standard physics in the early Universe. We apply this to [Equation D.4](#). We do not do any test for the case [Equation D.3](#), because for this case we need to consider M_B from local observations, which will automatically include the M_B tension (and consequently the Hubble tension) [30, 31]. In other words, for [Equation D.3](#), we cannot really break the degeneracy between these tensions and the violation of cosmic distance duality. In [Figure 6](#), we test this for the combination of DESI DR2 BAO, Union3 SNIa, and CMB data, and we find there is no evidence of distance duality violation. Note that here we used $r_d = (147.43 \pm 0.25)$ Mpc, from Planck+ACT DR6 CMB observations [2, 3], which is consistent with the DESI DR2 main paper [1].

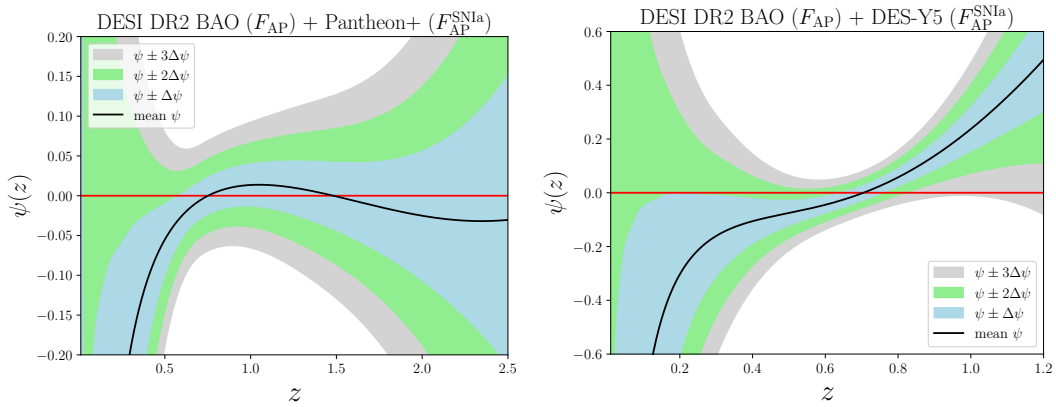


Figure 7. Test of standard candle assumptions, with no other violation of standard physics.

D.2 Violation of standard candle assumptions

Here we test whether there is any violation of the standard candle assumptions, i.e., any redshift dependence in M_B , which is equivalent to redshift dependence of α (see [Equation 2.3](#)).

We assume that distance duality holds. Rewriting [Equation 2.3](#) as

$$\alpha(z) = r_d \frac{\tilde{D}_M(z)}{A(z)}, \quad (\text{D.5})$$

we find that

$$\alpha'(z) = r_d \frac{[A(z)\tilde{D}'_M(z) - A'(z)\tilde{D}_M(z)]}{A^2(z)}. \quad (\text{D.6})$$

These two equations imply

$$\psi \equiv \frac{\alpha'}{\alpha} = \frac{\tilde{D}'_M}{\tilde{D}_M} - \frac{A'}{A} = \frac{1}{F_{\text{AP}}} - \frac{1}{F_{\text{AP}}^{\text{SNIa}}} \quad \text{with} \quad F_{\text{AP}}^{\text{SNIa}} = \frac{A}{A'}. \quad (\text{D.7})$$

Violation of the standard candle assumption corresponds to $\psi \neq 0$. This test is independent of r_d . The test is not directly applicable to Union3 data because there is no M_B parameter involved to be tested. [Figure 7](#) shows ψ for Pantheon+ (left) and DES-Y5 (right), combined with DESI DR2 data. It is evident that for Pantheon+, with $z < 0.5$, there is redshift evolution of M_B at slightly more than 1σ , but well within 1σ for $z > 0.5$. For DES-Y5, it is similar for lower redshift, but at around $z = 1$, there is up to 3σ evidence for redshift evolution of M_B . In other words, if there is no inconsistency coming from any other modification, then this is evidence for the violation of standard candle assumptions.

References

- [1] **DESI** Collaboration, M. Abdul Karim et al., *DESI DR2 Results II: Measurements of Baryon Acoustic Oscillations and Cosmological Constraints*, [arXiv:2503.14738](https://arxiv.org/abs/2503.14738).
- [2] **Planck** Collaboration, N. Aghanim et al., *Planck 2018 results. VI. Cosmological parameters*, *Astron. Astrophys.* **641** (2020) A6, [[arXiv:1807.06209](https://arxiv.org/abs/1807.06209)]. [Erratum: *Astron. Astrophys.* 652, C4 (2021)].
- [3] **ACT** Collaboration, M. S. Madhavacheril et al., *The Atacama Cosmology Telescope: DR6 Gravitational Lensing Map and Cosmological Parameters*, *Astrophys. J.* **962** (2024), no. 2 113, [[arXiv:2304.05203](https://arxiv.org/abs/2304.05203)].
- [4] D. Brout et al., *The Pantheon+ Analysis: Cosmological Constraints*, *Astrophys. J.* **938** (2022), no. 2 110, [[arXiv:2202.04077](https://arxiv.org/abs/2202.04077)].
- [5] D. Rubin et al., *Union Through UNITY: Cosmology with 2,000 SNe Using a Unified Bayesian Framework*, *Astrophys. J.* **986** (2025) 231, [[arXiv:2311.12098](https://arxiv.org/abs/2311.12098)].
- [6] **DES** Collaboration, T. M. C. Abbott et al., *The Dark Energy Survey: Cosmology Results with ~ 1500 New High-redshift Type Ia Supernovae Using the Full 5 yr Data Set*, *Astrophys. J. Lett.* **973** (2024), no. 1 L14, [[arXiv:2401.02929](https://arxiv.org/abs/2401.02929)].
- [7] **DESI** Collaboration, K. Lodha et al., *Extended Dark Energy analysis using DESI DR2 BAO measurements*, [arXiv:2503.14743](https://arxiv.org/abs/2503.14743).
- [8] S. Nesseris, Y. Akrami, and G. D. Starkman, *To CPL, or not to CPL? What we have not learned about the dark energy equation of state*, [arXiv:2503.22529](https://arxiv.org/abs/2503.22529).
- [9] M. Cortés and A. R. Liddle, *On DESI's DR2 exclusion of Λ CDM*, [arXiv:2504.15336](https://arxiv.org/abs/2504.15336).
- [10] B. R. Dinda and R. Maartens, *Physical vs phantom dark energy after DESI: thawing quintessence in a curved background*, *Mon. Not. Roy. Astron. Soc.* **542** (2025) L31–L35, [[arXiv:2504.15190](https://arxiv.org/abs/2504.15190)].

[11] S.-F. Chen and M. Zaldarriaga, *It's all Ok: curvature in light of BAO from DESI DR2*, *JCAP* **08** (2025) 014, [[arXiv:2505.00659](#)].

[12] S. L. Guedezounme, B. R. Dinda, and R. Maartens, *Phantom crossing or dark interaction?*, [arXiv:2507.18274](#).

[13] A. Leauthaud and A. Riess, *Looking beyond lambda*, *Nature Astron.* **9** (8, 2025) 1123, [[arXiv:2509.00359](#)].

[14] W. J. Wolf, P. G. Ferreira, and C. García-García, *Cosmological constraints on Galileon dark energy with broken shift symmetry*, [arXiv:2509.17586](#).

[15] C. L. Steinhardt, P. Phillips, and R. Wojtak, *Dark Energy Constraints and Joint Cosmological Inference from Mutually Inconsistent Observations*, [arXiv:2504.03829](#).

[16] S. Afroz and S. Mukherjee, *Hint towards inconsistency between BAO and Supernovae Dataset: The Evidence of Redshift Evolving Dark Energy from DESI DR2 is Absent*, [arXiv:2504.16868](#).

[17] A. Favale, A. Gómez-Valent, and M. Migliaccio, *Quantification of 2D vs 3D BAO tension using SNIa as a redshift interpolator and test of the Etherington relation*, *Phys. Lett. B* **858** (2024) 139027, [[arXiv:2405.12142](#)].

[18] E. O. Colgáin and M. M. Sheikh-Jabbari, *DESI and SNe: Dynamical Dark Energy, Ω_m Tension or Systematics?*, [arXiv:2412.12905](#).

[19] P. Mukherjee and A. A. Sen, *A New $\sim 5\sigma$ Tension at Characteristic Redshift from DESI-DR1 BAO and DES-SN5YR Observations*, [arXiv:2503.02880](#).

[20] M. Berti, E. Bellini, C. Bonvin, M. Kunz, M. Viel, and M. Zumalacarregui, *Reconstructing the dark energy density in light of DESI BAO observations*, *Phys. Rev. D* **112** (2025), no. 2 023518, [[arXiv:2503.13198](#)].

[21] M. Scherer, M. A. Sabogal, R. C. Nunes, and A. De Felice, *Challenging the Λ CDM model: 5σ evidence for a dynamical dark energy late-time transition*, *Phys. Rev. D* **112** (2025), no. 4 043513, [[arXiv:2504.20664](#)].

[22] Y. Wang and W. Lin, *Uncalibrated Cosmic Standards as a Robust Test on Late-time Cosmological Models*, *Astrophys. J.* **989** (2025), no. 1 120, [[arXiv:2506.04333](#)].

[23] G. Efstathiou, *Evolving dark energy or supernovae systematics?*, *Mon. Not. Roy. Astron. Soc.* **538** (2025), no. 2 875–882, [[arXiv:2408.07175](#)].

[24] **DES** Collaboration, M. Vincenzi et al., *Comparing the DES-SN5YR and Pantheon+ SN cosmology analyses: Investigation based on "Evolving Dark Energy or Supernovae systematics?"*, *Mon. Not. Roy. Astron. Soc.* **541** (2025), no. 3 2585–2593, [[arXiv:2501.06664](#)].

[25] F. Yang, X. Fu, B. Xu, K. Zhang, Y. Huang, and Y. Yang, *Testing the cosmic distance duality relation using Type Ia supernovae and BAO observations*, *Eur. Phys. J. C* **85** (2025), no. 2 186, [[arXiv:2502.05417](#)].

[26] T.-N. Li, G.-H. Du, P.-J. Wu, J.-Z. Qi, J.-F. Zhang, and X. Zhang, *Testing the cosmic distance duality relation with baryon acoustic oscillations and supernovae data*, [arXiv:2507.13811](#).

[27] F. Avila, F. Oliveira, C. Franco, M. Lopes, R. Holanda, R. C. Nunes, and A. Bernui, *Probing the Cosmic Distance Duality Relation via Non-Parametric Reconstruction for High Redshifts*, [arXiv:2509.07848](#).

[28] B. R. Dinda, *Minimal model-dependent constraints on cosmological nuisance parameters and cosmic curvature from combinations of cosmological data*, *Int. J. Mod. Phys. D* **32** (2023), no. 11 2350079, [[arXiv:2209.14639](#)].

[29] B. R. Dinda and R. Maartens, *Model-agnostic assessment of dark energy after DESI DR1 BAO*, *JCAP* **01** (2025) 120, [[arXiv:2407.17252](#)].

- [30] B. R. Dinda, *Cosmic expansion parametrization: Implication for curvature and H_0 tension*, *Phys. Rev. D* **105** (2022), no. 6 063524, [[arXiv:2106.02963](https://arxiv.org/abs/2106.02963)].
- [31] G. Efstathiou, *To H_0 or not to H_0 ?*, *Mon. Not. Roy. Astron. Soc.* **505** (2021), no. 3 3866–3872, [[arXiv:2103.08723](https://arxiv.org/abs/2103.08723)].